The Interaction between In-cylinder Flow and Flame Propagation in an Optical SI Engine Measured by High-Speed PIV

Yuji Ikeda[1,*]
1: i-Lab., Inc. KIBC 213 5-5-2 Minatojima-Minami, Chuo, Kobe, 650-0047 Japan
* Correspondent author: yuji@i-lab.net

Keywords: High speed PIV, Flame propagation, Planer laser tomography, SI engine

ABSTRACT

The relationship between the flow field and flame propagation is essential in determining the dynamics and effects of turbulent flow in an optical SI engine. In this study, the high-speed PIV technique was applied to evaluate the in-cylinder velocity and turbulence distribution under firing condition. The simultaneous measurement technique of in-cylinder flow and flame propagation characterized the relationship between flow field and flame propagation in the same cycle. A 500 cc single-cylinder optical engine was used for this experiment. The bore diameter and stroke length were 86 mm and 86 mm respectively, and compression ratio was 10.4. The flame front configuration was extracted from the PIV image based on planar laser tomography method. The strong contrast between the intensity of burned and unburned region in the captured images due to low gas and seed density of the former was utilized to derive this flame front. In order to evaluate the interaction between flame and flow with high resolution, the interrogation area was set to 16 × 16 pixels. This corresponds to 0.75 × 0.75 mm. The spatial filter of 6 mm was used to separate the instantaneous flow velocity into a low frequency component and a high frequency component. The engine speed was 1200 rpm and absolute intake pressure was 60 kPa. The equivalence ratio was stoichiometry condition. The ignition timing were set to 19 deg.BTDC. The characteristic cycles in the same test condition were extracted and discussed. The bulk flow with the large scale as large as the size of the combustion chamber influences the overall shape of the flame propagation, and the state of the flame propagation greatly fluctuates from cycle to cycle. The flame propagates with enhancing the large scale existing tumble flow that exists in earlier crank angle locations. Focusing on the local flame structure, the high-frequency velocity component was strong near the local flame peak and weak near the local flame valley. The flame at the local peak region propagates while pulling the valley region.

1. Introduction

The improvement of thermal efficiency, the reduction of fuel consumption and exhaust emission are strongly required for gasoline engine development. For that purpose, dilution of the air-fuel mixture and high EGR rate are effective methods. However, the cyclic variation of combustion increases for ultra-lean condition and high EGR rate conditions because the ignition and initial combustion instability increase and flame propagation speed decreases. In order to achieve stable ignition and initial combustion for even in ultra-lean condition, innovative ignition technologies have been required and developed (Alger et al., 2013; Shiraishi, 2012; Burrows et al., 2014; Weyand et al., 2014; Ikeda, 2014). On the other hand, the high tumble flow and squish flow are effective method to improve the flame propagation speed by higher turbulence. The turbulence and vortices of the in-cylinder flow enhances the flame surface area and this leads to increasing the flame propagation speed and burning velocity. Therefore, the interaction between in-cylinder flow and flame propagation needs to be understand in detail (Dierksheide et al., 2001; Dierksheide et al., 2002; Gindele et al.,1998; Geis et al., 2002; Krauseet. al., 2005; Lang et al., 2002; Voges et al., 2007; Westerweel, 2000).

Many successful approaches for measuring the flow field in internal combustion engines have been reported (Koehler et al., 2014; Cao et al., 2014; Lemétayer et al., 2014; Nishiyama et al.; 2014; Chen et al., 2015; Greene et. al., 2015; Miles et al., 2009; Zentgraf et al., 2014; Kegalj et al., 2008; Okura at al., 2014; Ikeda et al., 2012; Ikeda et al., 2016; Le et al., 2017). We applied high-speed PIV technique in order to measure and evaluate the in-cylinder flow under firing conditions to discuss not only the flow field during intake and compression stroke but also their effect on flame propagation under firing conditions. The results of the measurement techniques also enable the analysis of many more aspects regarding in-cylinder phenomena, some of which are shown in Fig. 1. For firing case, residual gas exists and its effect on flow field, such as mean flow, turbulence intensity and scale, as well as cyclic variation should be investigated. After the ignition timing, one of the most interesting topics is the effect of flow field on spark discharge,

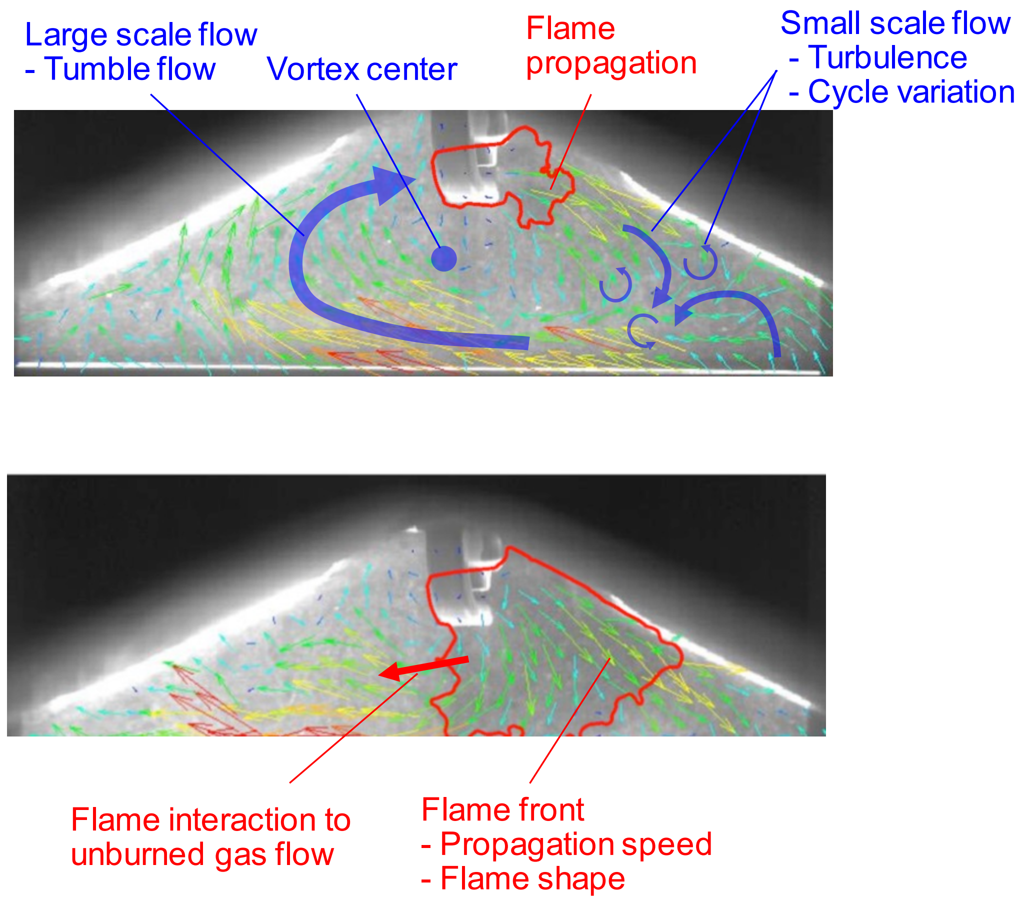

Fig. 1 Discussion items from simultaneous measurement of flow field and flame propagation by high speed PIV under firing condition

flame propagation speed, heat release and combustion duration. The large-scale flow will stretch the spark discharge and shift the propagating flame. The small-scale vortex will affect flame configuration and reaction zone thickness. The correlation between flow field and flame propagation in the same cycle can provide the clear indication of the optimum velocity and turbulence distribution in-cylinder to realize faster flame propagation and combustion.

In this study, the interaction between flow field and flame propagation was investigated in detail by using high-speed PIV under firing condition. The effects of large and small flow structure on flame propagation and configuration were discussed.

2. Experimental setup and experimental condition

Figure 1 shows the optical engine specifications and the optical measurement region of high-speed PIV measurement. The engine has a bore of 86 mm and stroke of 86 mm with a compression ratio of 10.4. Conventional gasoline fuel is delivered using a commercial port-fuel injection (PFI) system. The optical access into the combustion chamber of the engine is provided by a full quartz liner together with quartz windows on the top of the piston (54 mm diameter) and in the pent-roof. The measurement area was focus on the region near the spark plug in the bore center section. The flow distribution and initial flame were measured before and after the compressed TDC. Nd: YLF laser (maximum repetition frequency: 20 kHz) with a wavelength of 527 nm was used as a light source for high-speed PIV. Light from the laser is guided to the vicinity of the optical engine through the light guide arm. The laser beam at the tip of the guide arm is formed into a sheet with 2 mm thickness. The laser sheet is irradiated into the cylinder from the bottom via a mirror placed under the extended-piston. In order to visualize the flow and flame in the vicinity of the spark plug, we took images from the window of the pent-roof. The maximum frame speed of high-speed camera was 16,600 fps with full frame of 1280 × 800 pixels.

The solid particle with burning resistance was used as the seeding particle because the seeding is exposed in the combustion gas with high temperature. The traceability of this particle is enough for kHz order and has been proven by LDV measurement previously under similar engine operating condition.

In order to evaluate the interaction between flame and flow with high resolution, the interrogation area was set to 16 × 16 pixels. This corresponds to 0.75 × 0.75 mm. In this study, the spatial filter of 6 mm was used to separate the instantaneous flow velocity into a low frequency component and a high frequency component.

The flame surface was detected from the high-speed PIV images by distinguish the burned and unburned area. Signal intensity from the particles in the burned area was lower than that of unburned area because the density in the burned area was low. Therefore, the flame surface can be detected by Tomography technique. Compared to other simultaneous measurement such as LIF, it is possible to eliminate errors caused by the time and space mismatching during data integration because the flow distribution and the flame surface can be detected simultaneously from the same image.

The engine operating condition is shown in figure 2. The experiments were conducted under firing conditions. The engine speed was 1200 rpm and absolute intake pressure was 60 kPa. The equivalence ratio was stoichiometry condition. The ignition timing were set to 19 deg.BTDC.

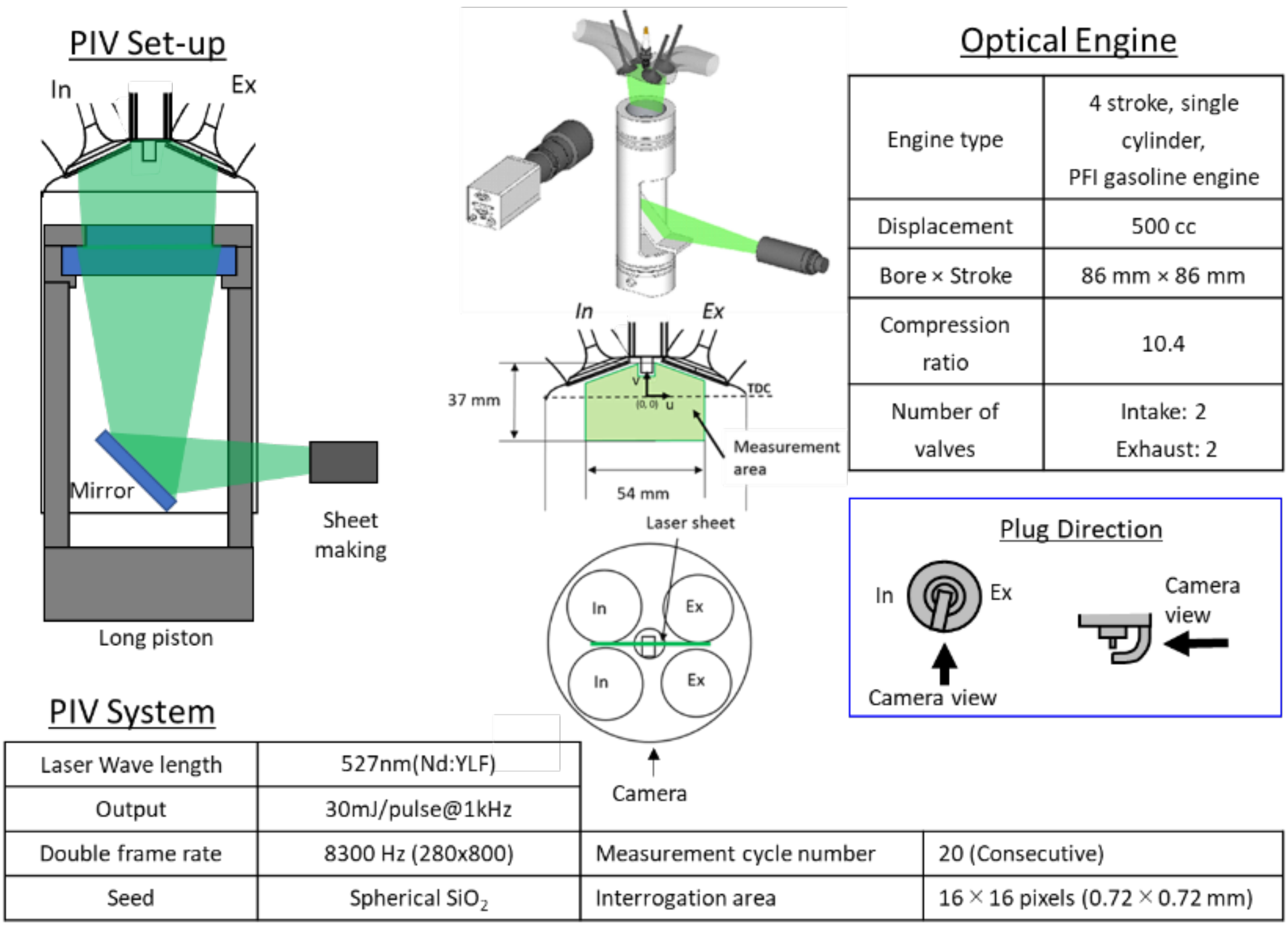

Optical Engine

Engine type	4 stroke, single cylinder, PFI gasoline engine
Displacement	500 cc
Bore × Stroke	86 mm × 86 mm
Compression ratio	10.4
Number of valves	Intake: 2 Exhaust: 2

PIV System

Laser Wave length	527nm(Nd:YLF)
Output	30mJ/pulse@1kHz
Double frame rate	8300 Hz (280x800)
Seed	Spherical SiO_2

Measurement cycle number	20 (Consecutive)
Interrogation area	16 × 16 pixels (0.72 × 0.72 mm)

Fig. 2 The optical engine specifications, the optical arrangement, and the measurement region of high-speed PIV measurement.

3. Results and discussion

Figure 3 and 4 show the flame development with the overlaid vectors of instantaneous flow and turbulence flow (high frequency component). Here, the characteristic cycles in the same test condition were extracted. Figure 3 shows a cycle (cycle A) in which the flame propagates symmetrically. On the other hand, Figure 4 shows a cycle (cycle B) in which the flame propagates with bias. In Fig. 3, there is no strong flow near the spark plug at the ignition timing and strong turbulence regions are scattered and distributed in the cylinder. After the ignition timing, the flame developed and propagated across the chamber in a symmetric fashion, almost like a spherical flame because of the absent of strong flow across the spark plug. The flame propagates with enhancing the large scale existing tumble flow that exists in earlier crank angle locations. The region of high flow velocity induced where the propagating flame joins the existing flow also results in a high turbulence region.

In Fig. 4, the center of the large-scale tumble flow from the intake and compression process is much closer to the spark plug. Therefore, the initial flame kernel generated following the flow enhances the flow on the front of the flame when the flame coincides with the tumble flow. In this case it can also be observed that when the flow moves toward the flame front, the flame propagation and growth is restricted where the flow is moving toward the flame front. The restrictions on flame propagation lasts quite a long time until the counter flow disappears. In this cycle, the region of the flame-front that experience the counter flow from tumble has very high turbulence level that lasted even when the flame front convolute and the flow has diminished.

As described above, the distribution of the bulk flow having the large scale as large as the size of the combustion chamber influences the overall shape of the flame propagation, and the state of the flame propagation greatly fluctuates from cycle to cycle. Next, the interaction between local flame structure and flow field of high frequency component was focused.

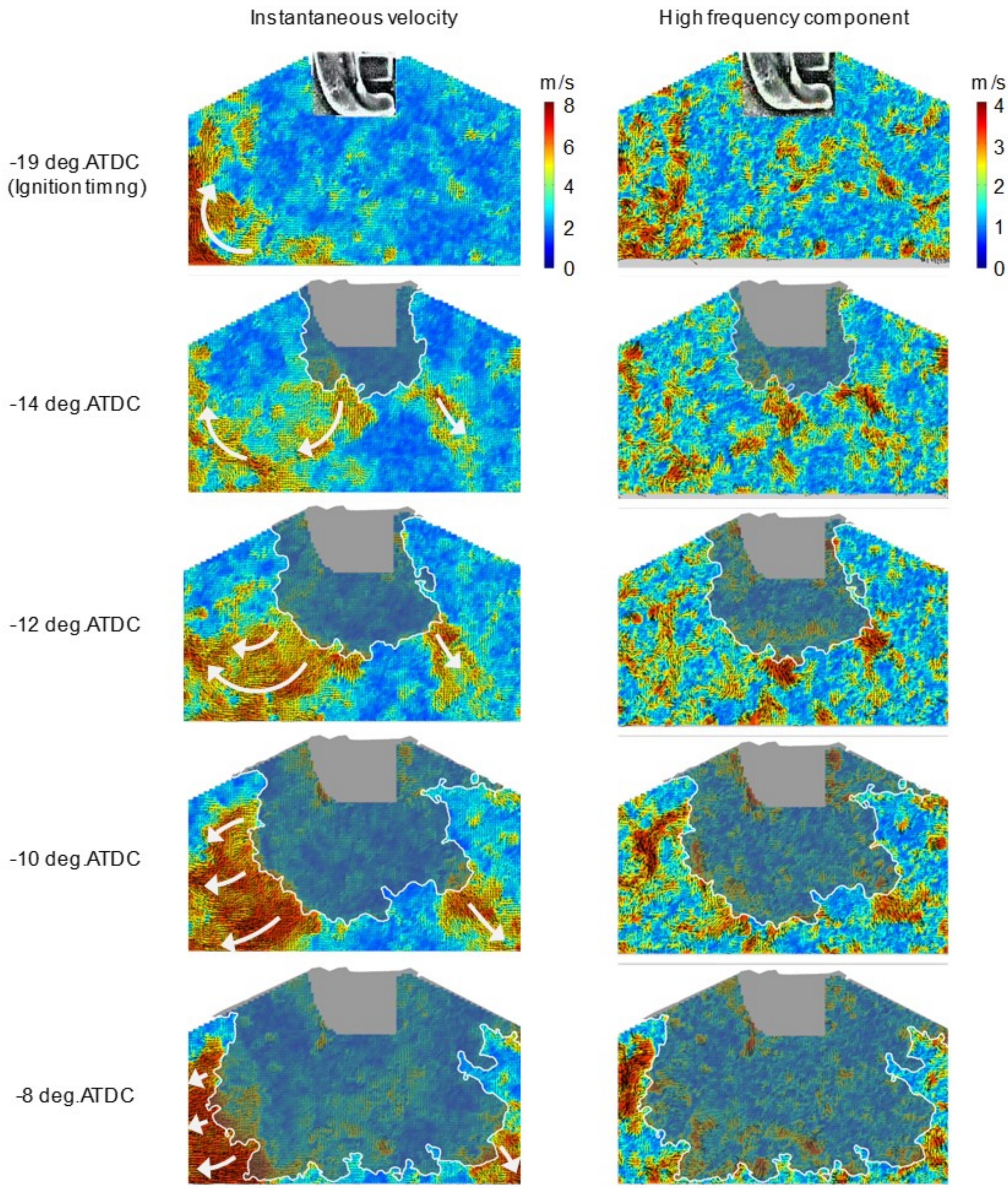

Fig. 3 Initial flame propagation and instantaneous velocity and turbulent field in cycle A (Engine speed: 1200 rpm, intake pressure: 60 kPa, equivalence ratio: 1.0)

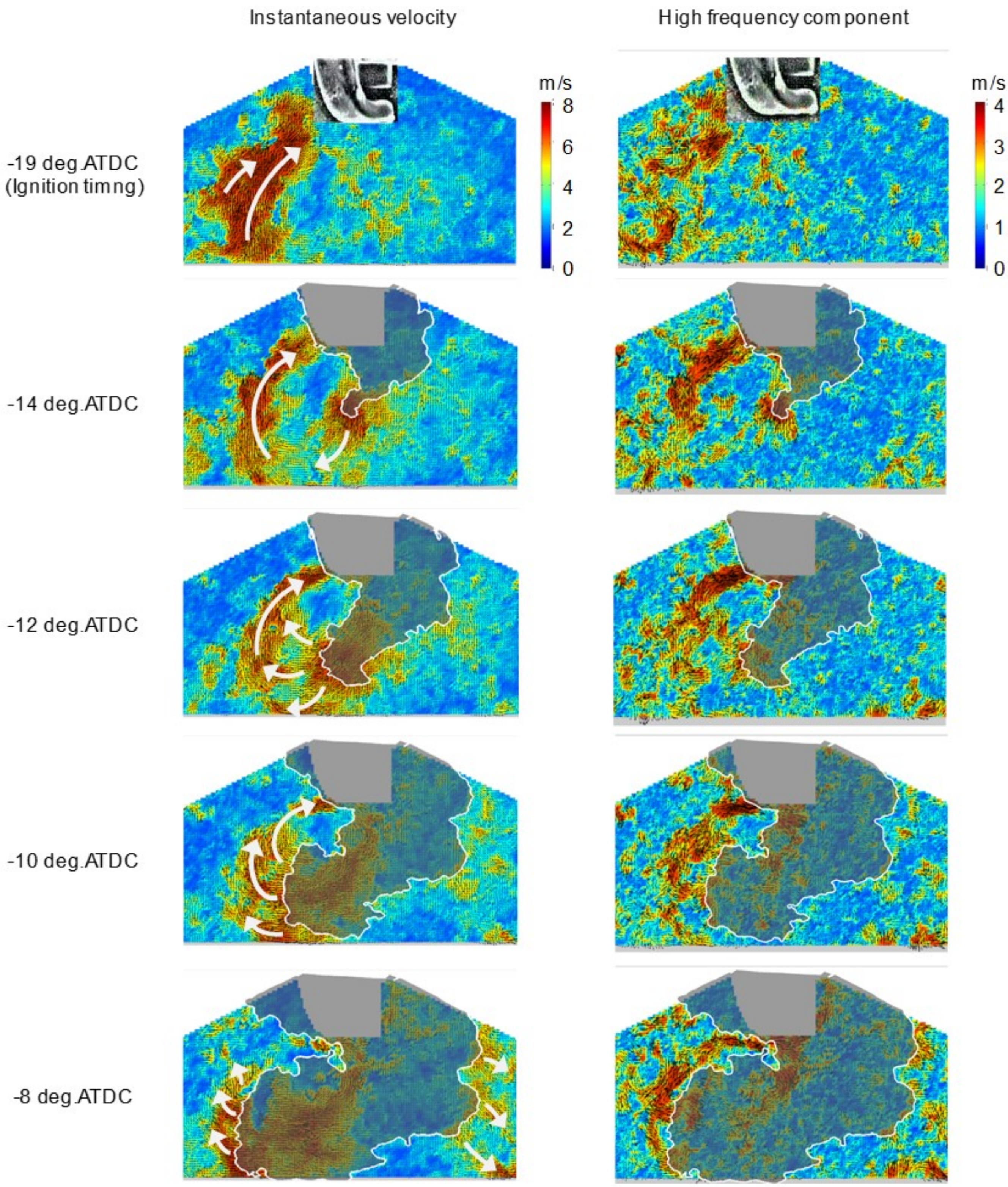

Fig. 4 Initial flame propagation and instantaneous velocity and turbulent field in cycle B (Engine speed: 1200 rpm, intake pressure: 60 kPa, equivalence ratio: 1.0)

Figure 5 shows the high-frequency component of flow velocity and the flame shape near the spark location of cycle A. Fig. 5 (a) shows the velocity distribution of the high-frequency component at -9 deg.BTDC. In this cycle, the overall flame propagation is almost symmetrically but the local flame shape is not smooth with several peaks and valleys. Here, the area of 7 mm x 14 mm surrounded by the white dotted line is the target area to be enlarged and investigated. Fig. 5 (b) and (c) shows the flame shape and velocity distribution in target area of cycle A at -9 and -8 deg.BTDC respectively. In Fig. 5 (b), the high-frequency velocity component was strong near the local flame peak and weak near the local flame valley. The flame at the local peak region propagates while pulling the valley region in Fig. 5 (c). Figure 6 shows the high-frequency component of flow velocity and the flame shape near the spark location of cycle B. In this cycle, the flame propagates with bias as a whole under the influence of the tumble flow. Here, the target area is 7.2 mm x 13.5 mm in the vicinity of the spark plug indicated by a white dashed line in Fig. 6 (a). The local flame shape was not smooth and there were several small peak and valley. Fig. 6 (b) and (c) shows the flame shape and velocity distribution in target area of cycle B at -9 and -8 deg.BTDC respectively. In Fig. 6 (b), the high-frequency velocity component was strong near the local flame peak and weak near the local flame valley as in Fig. 5 (b). In the lower half of the Fig. 6 (c), the flame at the local peak region propagated while pulling the valley region and the local valley region disappeared. In the upper half of the Fig. 6 (c) near the spark plug, the flame surface was pushed back to the unburned portion under the influence of the flow opposite to the propagation direction. The turbulence level of the unburned area is enhanced in these existing bulk flow stream as the flame propagates through them. Small scale eddies have a strong effect on flame curvatures and wrinkleless which can also help to push the flame propagation through difficult bulk-flow conditions.

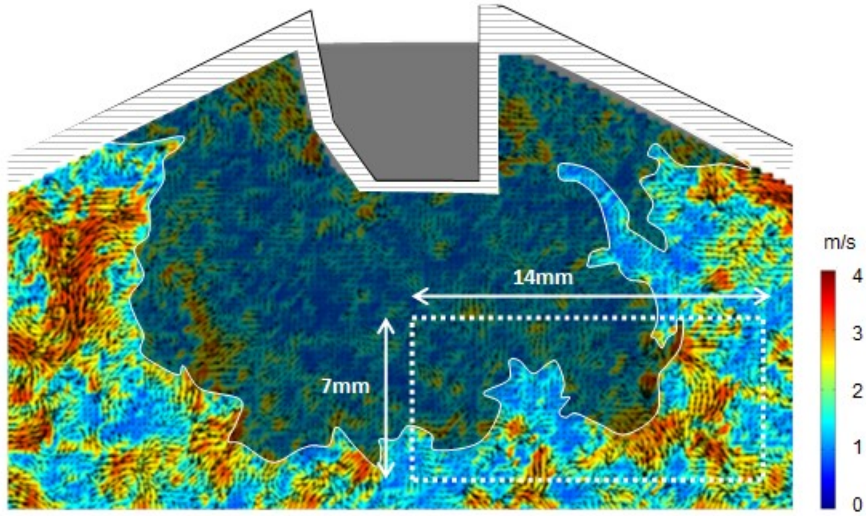

(a) Target area in cycle A

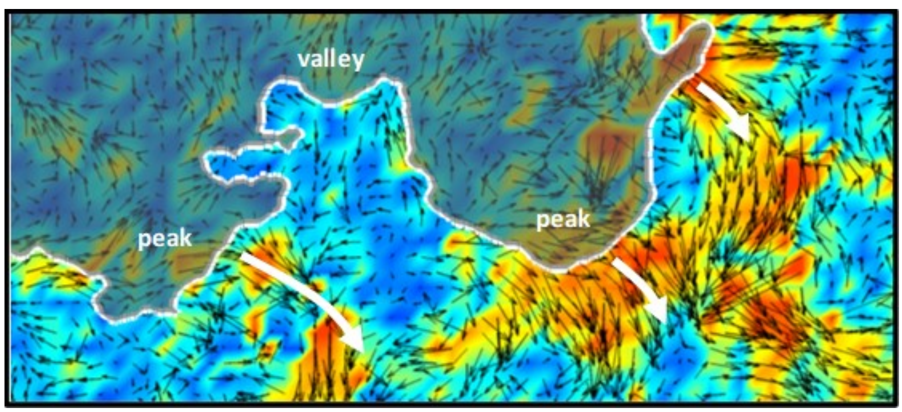

(b) Local instantaneous velocity and flame position at -9 deg.ATDC

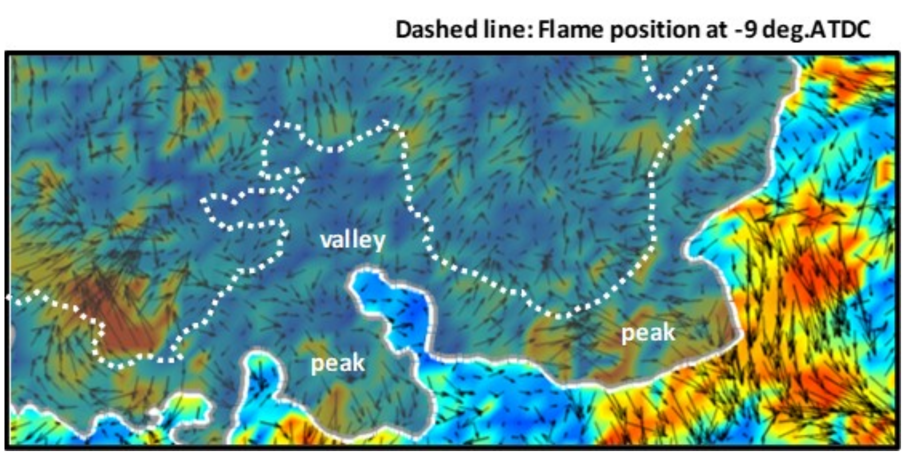

(c) Local instantaneous velocity and flame position at -8 deg.ATDC

Fig. 5 The Interaction between in-cylinder flow and flame propagation in cycle A

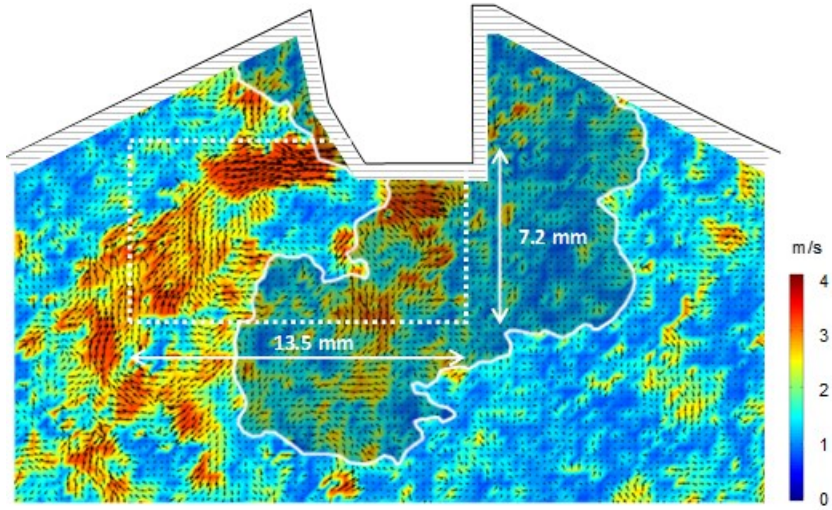

(a) Target area in cycle B

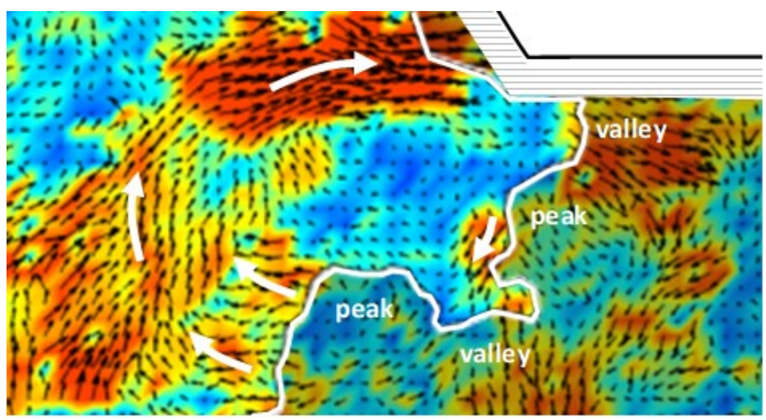

(b) Local instantaneous velocity and flame position at -9 deg.ATDC

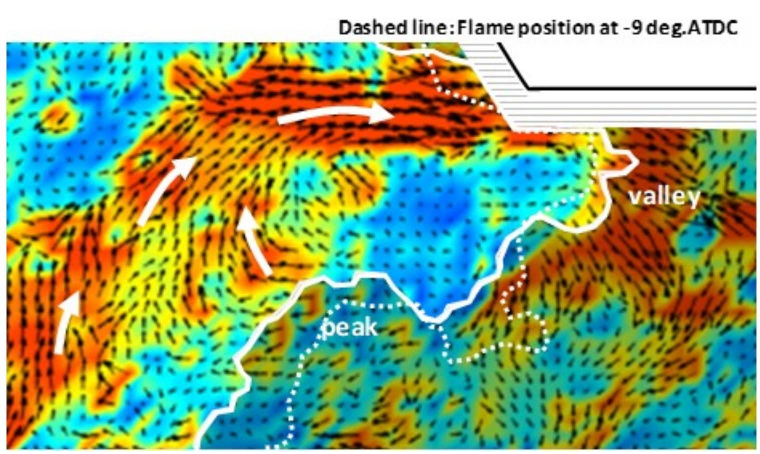

(c) Local instantaneous velocity and flame position at -8 deg.ATDC

Fig. 6 The Interaction between in-cylinder flow and flame propagation in cycle B

4. Conclusions

In this study, the interaction between in-cylinder flow and flame propagation was discussed. The in-cylinder flow field and flame propagation in an optical engine were measured simultaneously by high-speed PIV under firing condition. The bulk flow with the large scale as large as the size of the combustion chamber influences the overall shape of the flame propagation, and the state of the flame propagation greatly fluctuates from cycle to cycle. The flame propagates with enhancing the large scale existing tumble flow that exists in earlier crank angle locations. Focusing on the local flame structure, the high-frequency velocity component was strong near the local flame peak and weak near the local flame valley. The flame at the local peak region propagates while pulling the valley region.

References

Alger T., Gingrich J., Roberts B., Mangold B., & Sellnau, M. (2013). A high-energy continuous discharge ignition system for dilute engine applications. SAE Technical Paper, No. 2013-01-1628.

Burrows J. B., Mixell K., Reinicke P.B., Riess M., & Sens, M. (2014). Corona ignition – Assessment of physical effects by pressure chamber, rapid compression machine, and single-cylinder engine testing. 2nd International Conference on Ignition Systems for Gasoline Engines.

Cao Y., Thomas L., Borée J., & Guilain, S. (2014). Sensitivity study of cycle-to-cycle variation to air filling parameters of a SI engine. 17th Int Symp on Applications of Laser Techniques to Fluid Mechanics, Lisbon Portugal. 07-10 July.

Chen H., & Sick V. (2015). Plenoptic particle tracking velocimetry for internal combustion engine measurements. 11th International Symposium on Particle Image Velocimetry – PIV15, Santa Barbara, California, September 14-16.

Dierksheide, U., Meyer, P., Hovestadt, T. & Hentschel, W. (2001). Endoscopic 2D-PIV flow field measurements in IC engines. 4th International Symposium on Particle Image Velocimetry, Göttingen, Germany, September, PIV'01 Paper 1060.

Dierksheide, U., Meyer, P., Hovestadt, T. & Hentschel, W. (2002). Endoscopic 2D particle image velocimetry (PIV) flow field measurements in IC engines. Experiments in Fluids, 2002. 33(6),: p. 794-800.

Geis, T., Rottenkolber, G., Dittmann, M., Richter, B., Dullenkopf, K., & Wittig, S. (2002). Endoscopic PIV measurements in an enclosed rotor-stator system with pre-swirled cooling air. Proceedings of the 11th International symposium on application of laser techniques to fluid mechanics, Lisbon, Portugal, July

Gindele, J., & Spicher, U. (1998). Investigation of In-Cylinder Flow inside IC Engines using PIV with Endoscopic Optics. Proceedings of the 9th International symposium on application of laser techniques to fluid mechanics, Lisbon, Portugal, July

Greene M., Reuss D., & Sick, V. (2015). Near-wall flow measurements in a canonical internal combustion engine. 11th International Symposium on Particle Image Velocimetry – PIV15, Santa Barbara, California, September 14-16.

Ikeda Y. (2014). Development a microwave plasma ignition system with semiconductor microwave oscillator and combustion improvement in a practical SI engine. 2nd International Conference on Ignition Systems for Gasoline Engines.

Ikeda Y., Furui T., Le M K., & Nishiyama, A. (2016). In-Cylinder Flow Measurement in SI Engine under Firing Conditions by High Speed PIV, 18th Int Symp on Applications of Laser Techniques of Fluid Mechanics, Lisbon, Portugal.

Ikeda Y., Nishiyama A., Furui T., & Wachi Y. (2012). PIV/LDV combination for optimum turbulence generation scheme to spark ignition in wide operating condition of SI engine. 16th Int Symp on Applications of Laser Techniques to Fluid Mechanics, Lisbon Portugal, 09-12 July

Kegalj, M. & Schiffer, H.P. (2008). Endoscopic PIV Measurements in a Low Pressure Turbine Rig 14th International symposium on Applications of Laser Techniques to Fluid Mechanics Lisbon, Portugal, 07-10 July

Koehler M., Hess D., Kratzsch C., & Brücker, C. (2014). Flying PIV measurements in a driven IC engine flow. 17th Int Symp on Applications of Laser Techniques to Fluid Mechanics, Lisbon Portugal. 07-10 July.

Krause, N., Zähringer, K. & Pap., E. (2005). Time-resolved particle image velocimetry for the investigation of rotating stall in a radial pump Experiments in Fluids 39, pp192-201

Lang, H., Mørck, T., & Woisetschläger, J. (2002). Stereoscopic particle image velocimetry in a transonic turbine stage Experiments in Fluids, 32, pp 700-709

Le M K., Furui T., Nishiyama A., & Ikeda, Y. (2017). The Interaction of Flow-Field and Turbulence on Flame Development using High-Speed Combustion PIV, The Ninth International Conference on Modeling and Diagnostics for Advanced Engine Systems (COMODIA 2017), Okayama, Japan.

Lemétayer J., Cessou A., Domingues E., Lecordier B., & Lacour, C. (2014). Two-phase PIV to investigate spray/flow interaction in gasoline direct injection engine. 17th Int Symp on Applications of Laser Techniques to Fluid Mechanics, Lisbon Portugal. 07-10 July.

Miles P. C., RempelEwert B. H., & Reitz, R. D. (2009). Experimental assessment of a nonlinear turbulent stress relation in a complex reciprocating engine flow. Experiments in Fluids Volume 47, Issue 3, 451-461.

Nishiyama A., Furui T., & Ikeda, Y. (2014). Development of M12 Type Plug-in LDV Probe for Evaluation of Flow Field near Spark Location in SI Engine, 17th Int Symp on Applications of Laser Techniques of Fluid Mechanics, Lisbon, Portugal.

Okura Y., Segawa M., Onimaru H., Urata Y., & Tanahashi, M. (2014). Analysis of in-cylinder flow for a boosted GDI engine using high speed particle image velocimetry. 17th Int Symp on Applications of Laser Techniques to Fluid Mechanics, Lisbon Portugal. 07-10 July.

Shiraishi T. (2012). Possibility of the new ignition system using the low temperature plasma having dual function of strengthening ignition for SI combustion and promoting and controlling autoignition of HCCI combustion. 1st International Conference: Advanced Ignition System for Gasoline Engines.

Voges, M., Beversdorff, M., Willert, C. & Krain, H. (2007). Application of particle image velocimetry to a transonic centrifugal compressor Experiments in Fluids 43, pp371-384

Westerweel, J. (2000). Theoretical analysis of the measurement precision in particle image velocimetry Experiments in Fluids 29 S3-S12

Weyand P., Lorenz F., Schilling S., Bernhaerd B., Hofmann P., Graf J., & Hofherr, T. (2014). Adaptive continuous spark ignition as enabler for high dilution EGR operation. 2nd International Conference on Ignition Systems for Gasoline Engines.

Zentgraf F., Baum E., Böhm B., Dreizler A., & Peterson, B. (2014). Analysis of the turbulent in-cylinder flow in an IC engine using tomographic and planar PIV measurements. 17th Int Symp on Applications of Laser Techniques to Fluid Mechanics, Lisbon Portugal. 07-10 July.